

This item was submitted to Loughborough's Institutional Repository (<https://dspace.lboro.ac.uk/>) by the author and is made available under the following Creative Commons Licence conditions.



CC creative commons
COMMONS DEED

Attribution-NonCommercial-NoDerivs 2.5

You are free:

- to copy, distribute, display, and perform the work

Under the following conditions:

 **Attribution.** You must attribute the work in the manner specified by the author or licensor.

 **Noncommercial.** You may not use this work for commercial purposes.

 **No Derivative Works.** You may not alter, transform, or build upon this work.

- For any reuse or distribution, you must make clear to others the license terms of this work.
- Any of these conditions can be waived if you get permission from the copyright holder.

Your fair use and other rights are in no way affected by the above.

This is a human-readable summary of the [Legal Code \(the full license\)](#).

[Disclaimer](#) 

For the full text of this licence, please go to:
<http://creativecommons.org/licenses/by-nc-nd/2.5/>

Room-temperature atmospheric argon plasma jet sustained with submicrosecond high-voltage pulses

J. L. Walsh and M. G. Kong^{a)}

Department of Electronic and Electrical Engineering, Loughborough University, Loughborough, Leicestershire LE11 3TU, United Kingdom

(Received 9 December 2006; accepted 6 November 2007; published online 27 November 2007)

In this letter, an experimental study is presented to characterize a room-temperature plasma jet in atmospheric argon generated with submicrosecond voltage pulses at 4 kHz. Distinct from sinusoidally produced argon discharges that are prone to thermal runaway instabilities, the pulsed atmospheric argon plasma jet is stable and cold with an electron density 3.9 times greater than that in a comparable sinusoidal jet. Its optical emission is also much stronger. Electrical measurement suggests that the discharge event is preceded with a prebreakdown phase and its plasma stability is facilitated by the short voltage pulses. © 2007 American Institute of Physics.

[DOI: 10.1063/1.2817965]

Offering a unique chamberless route to wide-ranging surface chemistry near room temperature, atmospheric pressure glow discharges (APGDs) have found increasing use in numerous applications such as nanoscience,¹ biodecontamination,² and plasma display technology.³ One intrinsic feature of APGD is their tendency for the glow-to-arc transition, and so a key challenge in their development is to attain high plasma stability while maintaining efficient reaction chemistry.⁴ This can be addressed with a jet configuration in which the APGD is generated in a region of an inert gas and then flushed to a separate region of reactive gases for surface treatments, thus achieving high plasma stability and active reaction chemistry in spatially different locations.⁵⁻¹² When helium is used as the inert gas, such jet configurations are particularly effective in controlling plasma instabilities associated to the glow-to-arc transition. From an economics standpoint, however, it is desirable to realize APGD applications with less expensive inert gases such as argon.¹³ Yet, the use of argon has been found to considerably elevate the gas temperature of APGD jets,^{7,14-16} thus rendering their use for near room-temperature applications. One possible solution is to employ pulsed excitation, known to reduce electrical energy consumption and gas temperature.¹⁷ Studies of pulsed argon APGD are both interesting and timely, since most pulsed APGD have so far employed a helium-dominant working gas.¹⁸⁻²² In this letter, we report an experimental study of a room-temperature argon APGD jet achieved with repetitive submicrosecond high-voltage pulses at kilohertz frequencies.

The argon APGD jet was produced inside a quartz tube wrapped with a metal strip of 1 cm wide as the powered electrode and flushed in an atmospheric argon flow to a downstream dielectric sheet as the grounded electrode. The inner diameter of the quartz tube was 1.5 mm and the argon flow rate was 5 slm. The use of the quartz tube suggests that the generated plasma was effectively a dielectric-barrier discharge in atmospheric argon. The pulsed power supply was capable of delivering submicrosecond voltage pulses of up to 15 kV at frequencies up to 5 kHz.²⁰⁻²² For results presented

here, the excitation frequency was fixed to 4 kHz. The discharge current and the applied voltage were measured with a wideband current probe and a wideband voltage probe, respectively.

Figure 1 shows an optical emission spectrum around the OH line at 309 nm and an image of the argon APGD jet treating a human finger. Optical emission spectra were obtained using a spectrometer with a focal length of 0.3 m and a grating of 2400 grooves/mm, and the plasma image was taken with an exposure time of 50 ms using an intensified charge coupled device camera. The measured emission spectrum was compared to theoretical spectra simulated at different gas temperatures using LIFBASE,²³ and the best fit as determined by Pearson's χ^2 test was found to be with a gas temperature of 320 K. A 2.5% error bar is indicated on the simulated spectrum at 320 K in Fig. 1, which also shows the simulated spectrum with 420 K. As an alternative temperature measurement, a thermometer with a nominal error of 1 °C was placed in the plasma plume near the jet nozzle and the average from three independent readings was 28.0 ± 0.3 °C. This is considerably lower than the minimum gas temperature of 450 K reported so far for atmospheric argon plasmas.^{7,14-16} The pulsed Ar plasma jet can operate continuously for many hours without any marked temperature rise, suggesting an effective suppression of any thermal

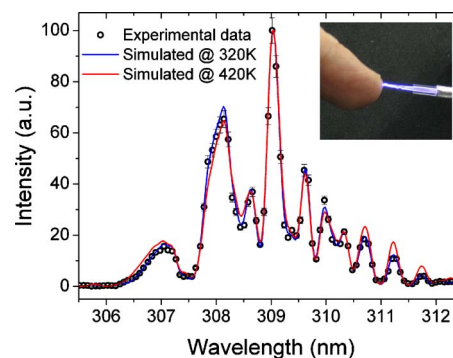


FIG. 1. (Color online) Measured and simulated optical emission spectra around the OH line at 309 nm for the submicrosecond pulsed atmospheric argon plasma jet. The inset shows the APGD jet with a human finger as the grounded electrode. The error bars on the 320 K simulated spectrum represents 2.5%.

^{a)} Author to whom correspondence should be addressed. Electronic mail: m.g.kong@lboro.ac.uk

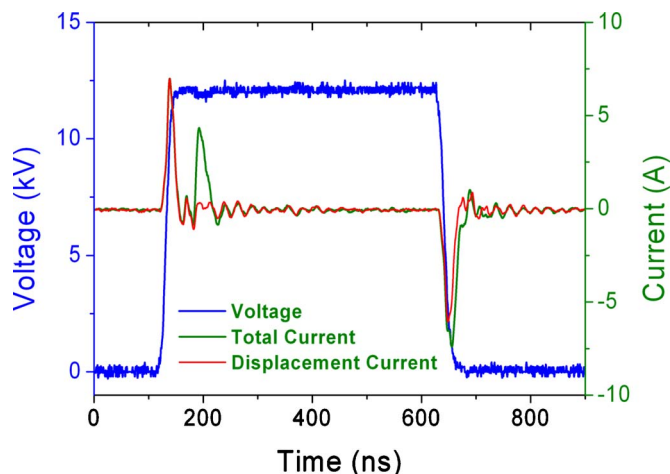


FIG. 2. (Color online) Traces of the applied voltage, the total discharge current and the displacement current of the submicrosecond pulsed argon APGD jet.

runaway instabilities. The pulsed jet in Fig. 1 is therefore a room-temperature atmospheric argon plasma and useful in widening the diversity range of applications that can benefit from atmospheric argon plasmas. It is known that very small electrode structures combined with very high gas flow rates help reduce gas temperature in atmospheric plasmas, but this approach tends to result in variation in cycle-to-cycle plasma properties. The pulsed atmospheric Ar plasma jet does not rely on high flow rates of the background gas, and its electrical and optical properties have an excellent cycle-to-cycle repeatability.

Current and voltage of the pulsed atmospheric Ar plasma jet are shown in Fig. 2 for which the peak applied voltage is 12 kV; the voltage pulsewidth measured as full width at half maximum is 505 ns. The rise time and the fall time of the applied voltage pulse are very short at 15 and 22 ns, respectively, causing one large displacement current to be established at each of the voltage-rising and the voltage-falling edges. Their peaks are, respectively, 7.0 and -6.0 A at 138 ns and 648 ns, at which the corresponding total current peaks are 7.0 and -7.5 A. In addition, the total current reaches a peak of 4.5 A at 192 ns where the main discharge event occurs. It is of interest to note that the current peak of 4.5 A occurs some 75 ns after the onset of the voltage pulse at 117 ns. This delay is likely to be related to a prebreakdown phase in which a weak Townsend discharge takes place to accumulatively increase surface charges on the quartz tube wall and subsequently elevate the local electric field above the threshold for gas breakdown. The delay of the current pulse from the onset of the voltage pulse was also observed in submicrosecond pulsed APGD between two parallel bare electrodes.^{21,22}

Following the prebreakdown phase, the 4.5 A current pulse reaches its peak and then falls to form a nanosecond pulse of 33 ns from 182 to 215 ns even though the applied voltage remains at 12 kV. This is because the electrons generated inside the quartz tube travel to and arrive at the inner wall of the quartz tube, and the resulting voltage across the quartz tube wall is at the opposite direction to the applied voltage thus reducing the gas voltage. Consequently, the ionization process is stopped to cause the fall in the discharge current. This is typical of dielectric barrier discharges¹³⁻¹⁷ and the duration of the current pulse is largely determined by

the electron transition time from the middle of the gas gap to the dielectric.²⁴ In addition, current growth is controlled by the very short pulsewidth of the submicrosecond voltage pulses. In other words, plasma instabilities are controlled by the short pulsewidth of the voltage pulses and this control is further assisted by a dielectric-barrier discharge mechanism.

It is worth comparing plasma generation in the pulsed Ar jet with that in a conventional sinusoidal Ar plasma jet. Given its very short current pulse, we assume that electrons generated in the pulsed Ar jet remained uncollected by the quartz tube wall during the 33 ns of the 4.5 A current pulse. This equals a space-averaged electron density of $2.6 \times 10^{13} \text{ cm}^{-3}$ if the plasma volume is approximated by an electrode length of 1 cm multiplied by a circular cross-section area of 1.77 mm^2 in diameter. As a comparison, we used the same apparatus but with a 4 kHz sinusoidal voltage of 20 kV peak to peak, the resulting current pulse had a peak of 130 mA and a pulsewidth of 300 ns. Again, assuming electrons in the 300 ns current pulse did not reach the quartz wall, the space-averaged electron density was found to be $6.8 \times 10^{12} \text{ cm}^{-3}$, a factor of 3.9 lower than that generated in the pulsed Ar jet. In practice, some generated electrons may reach the quartz wall. The resulting electron loss is less significant in the pulsed case due to its much shorter current pulse and so the electron density ratio is likely to be even more than 3.9. This suggests that the pulsed atmospheric Ar plasma jet is capable of greater plasma generation at lower gas temperature than its sinusoidal counterpart.

As the gas voltage is reduced below the breakdown voltage after the current pulse, electrons generated during the gas breakdown are either stored on the wall of the quartz tube or left drifting inside the tube. The drifting electrons can, in principle, be carried by the argon flow to reach the grounded electrode and register a small current peak. To assess this possibility, we performed a two-dimensional electrostatic computation of the electrode structure of Fig. 1 using a commercial software. At an applied voltage of 12 kV, the electric field in the passage of the Ar flow was found at about 7.2–10.8 kV/cm at which the electron drift velocity was estimated to be about $(2-3) \times 10^6 \text{ cm/s}$ in atmospheric argon.²⁵ As the nozzle side of the powered electrode is 1.5 cm away from the ground electrode, an electron is likely to take at least 500 ns to travel from the plasma generating region to the grounded electrode. This is markedly longer than the interval of 398 ns from the end of the 4.5 A current pulse to the beginning of the voltage pulse fall. Therefore, the drifting electrons cannot reach the grounded electrode to register a current pulse before the fall of the voltage pulse. At the fall of the voltage pulse, they add to the displacement current pulse to increase slightly the total current pulse. This is consistent with the observation of Fig. 2.

The above interpretation can be further supported by changing the applied voltage. As the applied voltage decreases, the onset of the current pulse should occur at a more delayed instant from the onset of the voltage pulse because a longer prebreakdown phase is needed to arrive at the threshold for gas breakdown. Figure 3 shows the traces of the conduction current obtained by subtracting the displacement current from the total current at an applied voltages of 13.3, 11.4, and 9.4 kV for which the current pulse occurs at a progressively delayed point from the onset of the voltage pulse. This confirms that the main discharge event is indeed preceded by a prebreakdown phase. It is also worth noting

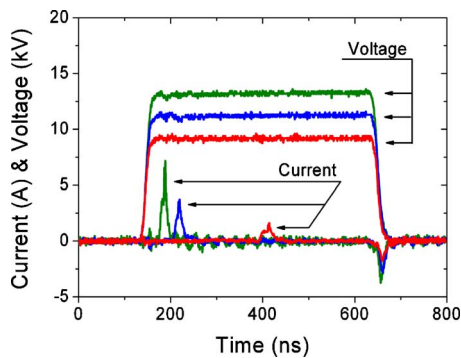


FIG. 3. (Color online) Traces of the applied voltage and the conduction current of the submicrosecond pulsed argon APGD jet at 4 kHz, at three different values of the peak applied voltage.

that the peak discharge current in Fig. 3 is larger at larger applied voltage, but with a narrower pulsewidth. This is because a larger applied voltage leads to the production of more electrons and hence a larger discharge current. In addition, the availability of more electrons at a larger applied voltage results in a more rapid charging of the quartz tube and faster reduction of the gas voltage to reduce the discharge current. Consequently, a narrow pulse of large discharge current is established, as shown in Fig. 3. Power consumption in the pulsed APGD jet was about 0.8–1.6 W for the three cases in Fig. 3, much smaller than that in atmospheric argon jets reported so far.^{7,14–16}

Figure 4 shows the optical emission spectrum of the Ar pulsed APGD jet at 11.4 kV and its sinusoidal counterpart with a peak-to-peak applied voltage of 20 kV, in which clear emission lines are seen of hydroxyl at 309 nm and atomic oxygen at 777 nm. Nitrogen and oxygen lines were present because the argon jet was flushed into the downstream ambient air. Distinctive from helium APGD jets of which the optical emission spectra are dominated by nitrogen lines,²⁰ Fig. 4 is dominated by numerous argon lines particularly

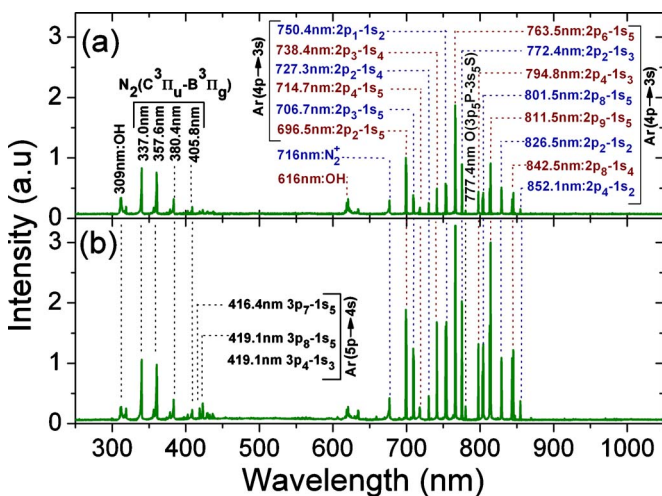


FIG. 4. (Color online) Optical emission spectrum of (a) a sinusoidally excited atmospheric Ar jet with a peak-to-peak voltage of 20 kV and (b) the submicrosecond pulsed argon APGD jet at 11.4 kV, both at 4 kHz.

related to $4p \rightarrow 4s$ and $5p \rightarrow 4s$ transitions (Paschen notation).²⁶ These are much stronger in the pulsed case with the intensity ratio of the pulsed-to-sine cases being 1.85, 1.74, and 3.33 for the three strongest Ar lines at 696.5, 763.5, and 811.5 nm. The pulsed-to-sine intensity ratio for the atomic oxygen line at 777 nm is similarly large at 3.3. The stronger optical emission of the pulsed Ar jet in Fig. 4 is consistent with its larger electron density estimated from Fig. 2.

In summary, we have shown that a room-temperature atmospheric argon plasma jet can be generated with submicrosecond voltage pulses at kilohertz frequencies. Plasma instabilities in the pulsed APGD jet were controlled effectively by the very short pulsewidth of the submicrosecond voltage pulses and further assisted by a dielectric-barrier discharge mechanism. Plasma generation is also more efficient in the pulsed case compared to its sinusoidal counterpart, as indicated by an electron density ratio of 3.9 and an optical intensity ratio of 3.3 at the atomic oxygen line at 777 nm.

This work was supported by the Engineering and Physical Sciences Research Council, UK.

¹H. Shirai, T. Kobayashi, and Y. Hasegawa, Appl. Phys. Lett. **87**, 143112 (2005).

²X. T. Deng, J. J. Shi, and M. G. Kong, IEEE Trans. Plasma Sci. **34**, 1310 (2006).

³J. G. Eden and S. J. Park, Phys. Plasmas **13**, 057101 (2006).

⁴J. J. Shi and M. G. Kong, Appl. Phys. Lett. **87**, 201501 (2005).

⁵K. Inomata, H. Ha, K. A. Chaudhary, and H. Koinuma, Appl. Phys. Lett. **64**, 46 (1994).

⁶S. E. Babayan, J. Y. Jeong, V. J. Tu, J. Park, G. S. Selwyn, and R. F. Hicks, Plasma Sources Sci. Technol. **7**, 286 (1998).

⁷S. Wang, V. Schulz-von der Gathen, and H. F. Dobeles, Appl. Phys. Lett. **83**, 3272 (2003).

⁸A. P. Yalin, Z. Q. Yu, O. Stan, K. Hoshimiya, A. Rahman, V. K. Surla, and G. J. Collins, Appl. Phys. Lett. **83**, 2766 (2003).

⁹W. C. Zhu, B. R. Wang, Z. X. Yao, and Y. K. Pu, J. Phys. D **38**, 1396 (2005).

¹⁰X. T. Deng, J. J. Shi, G. Shama, and M. G. Kong, Appl. Phys. Lett. **87**, 153901 (2005).

¹¹M. Laroussi and X. Lu, Appl. Phys. Lett. **87**, 113902 (2005).

¹²Y. C. Hong and H. S. Uhm, Appl. Phys. Lett. **89**, 221504 (2006).

¹³N. Gherardi and F. Massines, IEEE Trans. Plasma Sci. **29**, 536 (2001).

¹⁴T. Ichiki, R. Taura, and Y. Horiike, J. Appl. Phys. **95**, 35 (2004).

¹⁵Y. Shimizu, T. Sasaki, T. Ito, K. Terashima, and N. Koshizaki, J. Phys. D **36**, 2940 (2003).

¹⁶D. Czynkowski, M. Jasinski, J. Mizerczyk, and Z. Zakrzewski, Czech. J. Phys. **56**, B684 (2006).

¹⁷M. G. Kong and X. T. Deng, IEEE Trans. Plasma Sci. **31**, 7 (2003).

¹⁸X. P. Lu and M. Laroussi, J. Appl. Phys. **98**, 023301 (2005).

¹⁹X. P. Lu and M. Laroussi, J. Phys. D **39**, 1127 (2006).

²⁰J. L. Walsh, J. J. Shi, and M. G. Kong, Appl. Phys. Lett. **88**, 171501 (2006).

²¹J. L. Walsh, J. J. Shi, and M. G. Kong, Appl. Phys. Lett. **89**, 161505 (2006).

²²J. L. Walsh and M. G. Kong, Appl. Phys. Lett. **89**, 231503 (2006).

²³J. Luque and D. R. Crosley, SRI International Report MP No. 99-009, 1999 (unpublished).

²⁴X. T. Deng and M. G. Kong, IEEE Trans. Plasma Sci. **32**, 1709 (2004).

²⁵V. Lisovski, J.-P. Booth, K. Landry, D. Douai, V. Cassagne, and V. Yegorenkov, J. Phys. D **39**, 660 (2006).

²⁶G.-B. Zhao, M. D. Argyle, and M. Radosz, J. Appl. Phys. **101**, 033303 (2007).